Advanced Materials Research Vol. 845 (2014) pp 421-425
Online available since 2013/Dec/04 at www.scientific.net

doi:10.4028/www.scientific.net/AMR.845.421

Visible-Light Photodegradation of Diisopropanolamine using Bimetallic Cu-Fe/TiO_2 photocatalyst

Raihan Mahirah Ramli[1,a], Fai Kait Chong[2,b] and Abdul Aziz Omar[1,c]

[1] Department of Chemical Engineering, Universiti Teknologi PETRONAS, 31750 Tronoh, Perak, Malaysia.
[2] Department of Fundamental & Applied Sciences, Universiti Teknologi PETRONAS, 31750 Tronoh, Perak, Malaysia.
[a]raihanmahirah@gmail.com, [b]chongfaikait@petronas.com.my, [c]aaziz_omar@petronas.com.my

Keywords: Copper-iron, Diisopropanolamine, Photodegradation, TiO_2, Visible-light

Abstract. Titania nanoparticles, TiO_2 were synthesized via microemulsion method prior to monometallic (Fe, Cu) or bimetallic (Cu−Fe) incorporation using wet impregnation method. The prepared photocatalysts were characterized using X-ray diffraction, field emission scanning electron microscopy, diffuse reflectance UV-Vis spectroscopy and point of zero charge. The addition of metals, especially Cu enhanced the absorbance in the visible region. The lowest band gap was observed for the bimetallic Cu-Fe/TiO_2 (2.77 eV) compared to bare TiO_2 (3.05 eV). The performance of the photocatalysts for photodegradation of diisopropanolamine (DIPA) at pH 8 was determined using a batch glass reactor under simulated sunlight (980 W/m^2). The best performance was displayed by Cu-Fe/TiO_2 with the highest DIPA removal of 92%.

Introduction

Alkanolamines such as diisopropanolamine (DIPA) was characterized having low biodegradability and high ecotoxicity [1]. Heterogeneous photocatalytic process employing semiconductor photocatalysts such as TiO_2, WO_3, and Fe_2O_3 displayed high efficiency in degrading a wide range of organic compounds into readily biodegradable compounds. Titania, TiO_2 attracted much interest compared to other photocatalysts due to its high photocatalytic activity, photostability and non toxicity [2,3]. Unfortunately, the drawback of TiO_2 is the high electron-hole ($e^-_{cb} - h^+_{vb}$) pair recombination rate which decreases its photocatalytic efficiency and poor absorption of visible light which represent almost 45% of the sunlight spectrum [4]. Therefore, considerable amount of research works have reported on the modification of TiO_2 with enhanced performance. To date, several approaches have been adopted including doping TiO_2 with transition metals [5,6]. Among the dopants, iron (Fe) [7] and copper (Cu) [8] have attracted much attention due to their low cost, abundant availability and high photocatalytic activity. Mineralization of dye utilizing Fe/TiO_2 photocatalyst displayed superior photocatalytic efficiency compared to bare TiO_2 [9]. Similar observation was exhibited by Cu/TiO_2 [9]. Photodegradation of diethanolamine (DEA) [10] and 2-dimethylamino-2-methyl-1-propanol (DMAMP) [11] under UV light have been reported using TiO_2 photocatalyst but no similar record could be obtained on photodegradation of DIPA. In the present paper, TiO_2 nanoparticles was synthesized via microemulsion method then modified with Fe, Cu or Cu-Fe incorporation using wet impregnation method. The photocatalysts were characterized using XRD, SEM, DRUV-Vis and PZC. The photodegradation efficiency of aqueous DIPA solution under visible light was monitored based on total DIPA removal.

Experimental

Photocatalysts preparation. TiO_2 nanoparticles were synthesized using titanium isopropoxide as the starting material. Triton X-100 was used as a template during synthesis [12]. The white powdered material was calcined at 350°C for 1 h in order to remove residual organic entities and to produce anatase TiO_2 from the hydroxides. Predetermined amounts of Fe or/and Cu salts were dissolved in distilled water followed by slow addition to the TiO_2. The metal loadings were the optimum values selected based on our preliminary optimization work on Fe/TiO_2 (0.2wt%) and

Cu/TiO_2 (1.8wt%) monometallic systems. The suspension was stirred prior to evaporation of the solvent at 80°C in a water bath followed by overnight drying in an oven at 100°C. The dried powder was grinded and calcined at 450°C for 1 h duration. The photocatalysts prepared were $0.2Fe/TiO_2$, $1.8Cu/TiO_2$ and $1.8Cu\text{-}0.2Fe/TiO_2$. For comparison, bare TiO_2 was also recalcined at 450°C for 1 h duration.

Photocatalyst Characterization. The X-ray diffraction patterns of the photocatalysts were recorded using XRD (Bruker D8 Advance). The morphologies of the photocatalysts were examined using field emission scanning electron microscope (FESEM, Supra55VP). The extent of light absorption of the photocatalysts were recorded using the DRUV-Vis spectrophotometer (Shimadzu Spectrometer 3150). The point of zero charge (PZC) for each of the photocatalysts was determined using the mass titration method [13]. The amounts of photocatalyst added into water were 1.0, 5.0, 10.0 and 20.0 wt% where the limiting pH values were measured after 24 h equilibration.

DIPA photodegradation. Photodegradation of aqueous DIPA solution was conducted in a glass reactor and positioned below a 500 W halogen lamp giving 980 W/m^2 of illumination. The aqueous DIPA solution, preadjusted to pH 8, was mixed with the photocatalysts (2.000 g/L) and stirred in the dark for 2 h for equilibration (dark process). Then, photodegradation under irradiation (photoreaction) was conducted for another 4 h. The system's efficiency was determined using Eq. 1:

$$DIPA\ removal\ (\%) = \frac{DIPA_i - DIPA_f}{DIPA_i} \chi\ 100 \quad (1)$$

where $DIPA_i$ is the initial concentration (1000 ppm) and $DIPA_f$ is the final concentration at the end of the photodegradation study. Concentration of DIPA was determined using Agilent 1100 High Performance Liquid Chromatography (HPLC) at λ=215 nm, column used for the analysis was YMC Pack Polymer C18 (250.0 × 6.0 mm I.D.), mobile phase of 100 mM NaH_2PO_4 and 100 mM NaOH (60/40 v/v) with a flow rate of 1.0 mL/min.

Results and Discussions

Photocatalyst characterization. Fig. 1 depicts the XRD patterns of the photocatalyst samples. All diffraction peaks in the figure display typical characteristic peaks for anatase TiO_2 (JCPDS file no. 21-1272). No characteristic peaks relating to the presence of Cu− or Fe−species were observed which could be due to the high dispersion of metal species on TiO_2 surface [14].

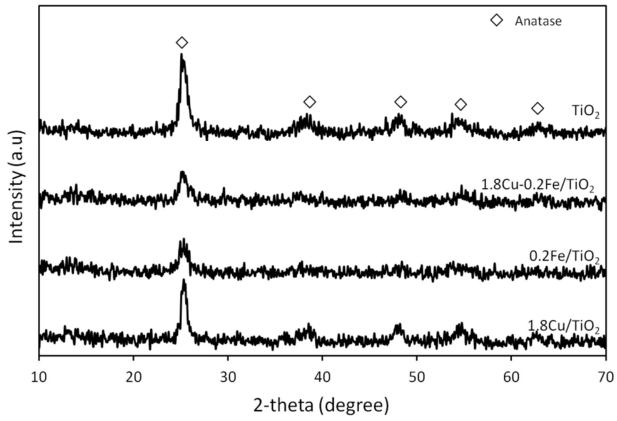

Fig. 1. XRD patterns of the prepared photocatalysts

The dominant peak at 25.3° was used to estimate the crystallite size of the photocatalyst using Debye Scherrer's equation. The highest crystallite size was displayed by bare TiO_2 (14.6 nm) while the smallest crystallite size was $0.2Fe/TiO_2$ (10.3 nm). On the other hand, both Cu/TiO_2 and $Cu\text{-}Fe/TiO_2$ photocatalysts containing 1.8 wt% Cu displayed larger crystallite sizes (14.2 nm and 12.6 nm, respectively) compared to $0.2Fe/TiO_2$. The increased in crystallite size may be ascribed to the increase in total metal loading. Meanwhile, the presence of Fe in $Cu\text{-}Fe/TiO_2$ may have prevented the agglomeration of the crystallites [14].

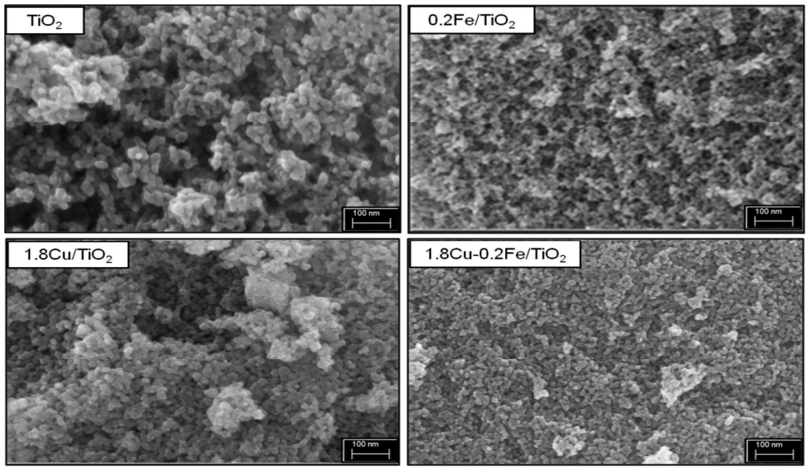

Fig.2. SEM micrographs of the prepared photocatalysts

All the photocatalysts display uniform spherical nanoparticles with different degree of agglomeration (Fig. 2). The particles of bare TiO_2 grown larger compared to the metal doped photocatalysts with average particle size of 13.8 nm. While 0.2Fe/TiO_2 photocatalyst shows average particle size of 12.4 nm with slight agglomeration caused for the small difference between XRD's crystallite size and SEM particle size measurement. The morphology of 1.8Cu/TiO_2 shows high agglomeration of particles, in agreement with the bigger crystallite size determined from XRD data. In contrast, less agglomeration could be observed for 1.8Cu-0.2Fe/TiO_2 photocatalyst. It could be suggested that the addition of Fe in the bimetallic photocatalyst has reduced the particles agglomeration leading to smaller particles compared to single Cu dopant [14]. While Fig. 3 presents the elemental mapping of bimetallic photocatalyst. The dopant metals Cu and Fe are highly dispersed and incorporated onto TiO_2 surface, explained the reason for undetectable peak related to these dopants in XRD analysis.

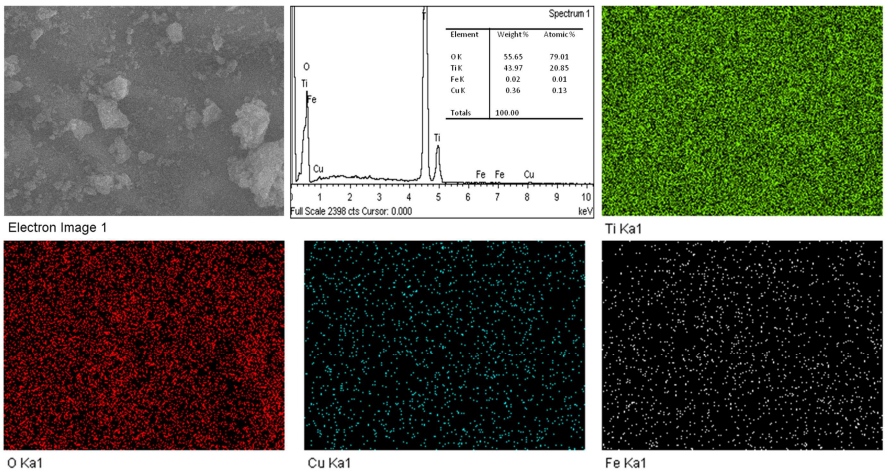

Fig. 3. EDX and mapping image of 1.8Cu-0.2Fe/TiO_2 photocatalyst

The DRUV-Vis spectra of the photocatalysts are depicted in Fig. 4(a). The absorption spectrum for bare TiO_2 shows an absorption edge at 400 nm corresponding to the band gap of 3.05 eV. The band gap can be calculated from Tauc plot [13], a plot of $[F(R).h\nu]^{1/2}$ versus photon energy ($h\nu$) as shown in Fig. 4(b). When the TiO_2 was doped with 0.2 wt% Fe, slight shift of the absorbance edge is observed which is in agreement with the colour change of the photocatalyst from white powder to yellowish due to the presence of Fe (Fig. 4(a)). Significant shift of the edge could be seen for 1.8Cu/TiO_2 while 1.8Cu-0.2Fe/TiO_2 displayed the largest shift.

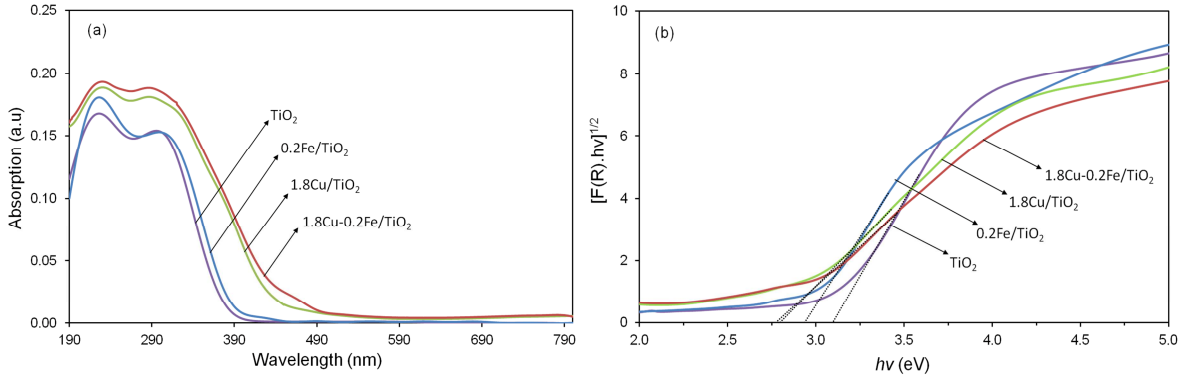

Fig. 4. (a) The DRUV-Vis absorption spectra and (b) plots of transformed Kubelka-Munk functions of the photocatalysts

The band gap of bare TiO_2 was 3.05 eV but upon incorporation of Fe (Fe/TiO_2), the value was reduced to 2.92 eV. The incorporation of Cu gave higher reduction to the band gap (2.78 eV) and that was reduced further for the codoped photocatalyst (2.77 eV). The blue shift in the absorption of photocatalysts suggested that the dopants successfully generate lower energy level between the valence and conduction bands [14]. For bare TiO_2, the PZC was observed at pH 9.9 while for $0.2Fe/TiO_2$, the value moves higher to pH 10.6. In contrast, photocatalysts doped with Cu and Cu-Fe displayed PZC in the acidic region with pH of 5.7 and 7.2, respectively. This PZC value is important in the photocatalytic oxidation of organic compounds especially in aqueous medium.

Photodegradation of aqueous DIPA solution. The degradation profile of DIPA is presented in Fig. 5. The lowest degradation is observed for unmodified TiO_2 (32.2%). When $0.2Fe/TiO_2$ was employed, the degradation efficiency of DIPA increased to 52.5%. This could be attributed to the higher absorption of the photocatalyst in the visible region (Fig. 4) which enables the material to absorp photon energy of the light for enhanced photocatalytic activity. Further enhancement is observed for $1.8Cu/TiO_2$ where 80% of DIPA was degraded within 2 h. This could be related to its PZC where at pH 8, Cu/TiO_2 photocatalyst surface was negatively charged while DIPA having pK_a value of 8.84 [15] was protonated. The electrostatic attraction between these two components increased the adsorption efficiency thus directly enhanced the photodegradation efficiency. Similar behaviour was also observed for the bimetallic $1.8Cu\text{-}0.2Fe/TiO_2$ (PZC at pH 7.2).

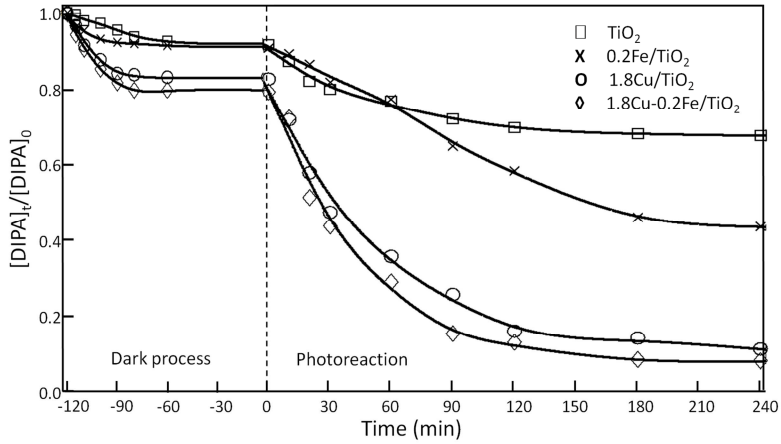

Fig. 5. Adsorption and photodegradation profile of DIPA using different photocatalysts

Another reason for this observation can be closely related to the photocatalysts properties. The crystallite size of codoped photocatalysts (70.13 m^2/g) was smaller compared to single Cu dopant (56.2 m^2/g), mean that its surface area is higher thus giving higher available sites for adsorption and degradation reaction to take place. Meanwhile, even though $0.2Fe/TiO_2$ photocatalyst has the highest surface area (88.42 m^2/g), the electrostatic repulsion between DIPA and the photocatalyst surface has markedly decreased the system's efficiency.

Conclusion

The incorporation of both 1.8 wt% Cu and 0.2 wt% Fe onto TiO_2 nanoparticles was found to enhance the synergistic effect from the two metals. The presence of Fe on Cu/TiO_2 was able to reduce the band gap of the bimetallic photocatalyst to 2.77 eV compared to the band gap of bare TiO_2 (3.05 eV). In addition, the extent of particles agglomeration in the bimetallic photocatalyst was also reduced. The XRD patterns did not reveal any diffraction peak relating to Cu- or Fe-species suggesting high dispersion of the materials on TiO_2. The bimetallic $1.8Cu\text{-}0.2Fe/TiO_2$ photocatalyst displayed the highest performance in DIPA photodegradation giving 92% of DIPA removal at pH 8.

References

[1] I. Eide-Haugmo, O.G. Brakstad, K.A. Hoff, K.R. Sørheim, E.F. da Silva, H.F. Svendsen, Environmental impact of amines, Energy Procedia 1(1) (2009) 1297-1304.
[2] D. Zhang, Enhanced photocatalytic activity for titanium dioxide by co-modification with copper and iron, Transition Metal Chemistry 35(8) (2010) 933-938.
[3] M.B. Fisher, D.A. Keane, P. Fernández-Ibáñez, J. Colreavy, S.J. Hinder, K.G. McGuigan, S.C. Pillai, Nitrogen and copper doped solar light active TiO_2 photocatalysts for water decontamination, App. Catal. B: Env. 130-131 (2013) 8-13.
[4] N. Riaz, F.K. Chong, B.K. Dutta, Z.B. Man, M.S. Khan, E. Nurlaela, Photodegradation of Orange II under visible light using $Cu–Ni/TiO_2$: Effect of calcination temperature, Chemical Engineering Journal 185-186 (2012) 108-119.
[5] X.L. Yuan, J.L. Zhang, M. Anpo, D. N. He, Synthesis of Fe^{3+} doped ordered mesoporous TiO_2 with enhanced visible light photocatalytic activity and highly crystallized anatase wall, Research on Chemical Intermediates 36 (2010) 83-93.
[6] L.S. Yoong, F.K. Chong, B.K. Dutta, Development of copper-doped TiO_2 photocatalyst for hydrogen production under visible light, Energy 34(10) (2009) 1652-1661.
[7] C.H. Lu, W.H. Wu, R.B. Kale, Microemulsion-mediated hydrothermal synthesis of photocatalytic TiO_2 powders, J. of Haz. Mat. 154(1-3) (2008) 649-654.
[8] M. Klare, J. Scheen, K. Vogelsang, H. Jacobs, J.A.C. Broekaert, Degradation of short-chain alkyl- and alkanolamines by TiO_2- and Pt/TiO_2-assisted photocatalysis, Chemosphere l41 (2000) 353-362.
[9] C.S. Lu, C.C. Chen, F.D. Mai, H.K. Li, Identification of the degradation pathways of alkanolamines with TiO_2 photocatalysis, J. of Haz. Mat. 165 (2009) 306-316.
[10] C.H. Lu, W.H. Wu, R.B. Kale, Microemulsion-mediated hydrothermal synthesis of photocatalytic TiO_2 powders, J. of Haz. Mat. 154(1-3) (2008) 649-654.
[11] J.S. Noh, and J.A. Schwarz, Estimation of the point of zero charge of simple oxides by mass titration, Journal of Colloid and Interface Science 130 (1989) 157-164.
[12] Y. Wu, J. Zhang, L. Xiao, F. Chen, Properties of carbon and iron modified TiO_2 photocatalyst synthesized at low temperature and photodegradation of acid orange 7 under visible light, Applied Surface Science 256(13) (2010) 4260-4268.
[13] A.B. Murphy, Band-gap determination from diffuse reflectance measurements of semiconductor films, and application to photoelectrochemical water-splitting, Sol. Energy Mat. and Sol. Cells 91 (2007) 1326-1337.
[14] Y. Wu, J. Zhang, L. Xiao, F. Chen, Preparation and characterization of TiO_2 photocatalysts by Fe^{3+} doping together with Au deposition for the degradation of organic pollutants, App. Catal. B: Env. 88 (2009) 525-532.
[15] E.S. Hamborg, G.F. Versteeg, Dissociation constants and thermodynamic properties of alkanolamines, Energy Procedia 1(1) (2009) 1213-1218.

Materials, Industrial, and Manufacturing Engineering Research Advances 1.1
10.4028/www.scientific.net/AMR.845

Visible-Light Photodegradation of Diisopropanolamine Using Bimetallic Cu-Fe/TiO_2 Photocatalyst
10.4028/www.scientific.net/AMR.845.421